Earthq Eng & Eng Vib (2012) 11: 257-268 **DOI**: 10.1007/s11803-012-0115-3

A study of local amplification effect of soil layers on ground motion in the Kathmandu Valley using microtremor analysis

Paudyal Y.R.[†], Yatabe R.[‡], Bhandary N.P.[§] and Dahal R.K.[§]

Geo-disaster Research Laboratory, Graduate School of Science and Engineering, Ehime University, Ehime, Matsuyama, Japan

Abstract: Past researchers have anticipated the occurrence of a great earthquake in the central Himalayas in the near future. This may cause serious damage in the Kathmandu Valley, which sits on an ancient lake bed zone, with lacustrine sediments of more than 500 m depth. In this study, the predominant frequency of ground motion is evaluated using the Horizontal-to-Vertical (*H/V*) spectral ratio technique and recordings of ambient noise. The results of the *H/V* ratio show two peaks in about 20 percent of the locations, which are distributed mainly in and around the center and northern part of the Kathmandu Valley. The predominant frequencies vary from 0.5 Hz to 8.9 Hz in the study area, whereas the second resonance frequency varies from 4 Hz to 6 Hz in the center and northern part of the valley. This indicates that the center and northern part of the valley have a wide range of resonance frequency due to two levels of impedance contrast − one may be from the surface layer and the other may be from the layer underneath. These two levels of resonance indicate the importance of considering the effects of surface and lower layers during the planning and designing of infrastructures in the Kathmandu Valley.

Keywords: microtremor; predominant frequency; resonance; Kathmandu Valley

1 Introduction

The Kathmandu Valley, where the capital of Nepal is located, falls in one of the most active tectonic zones of the Himalayan belt and has experienced many recurring destructive earthquakes in the past (Pandey *et al.*, 1995). Major historical earthquake damage in the valley was reported in 1255, 1408, 1681, 1803, 1810, 1833 and 1866 (Bilham *et al.*, 1995; Chitrakar and Pandey, 1986; Pandey *et al.*, 1995), while the latest strong shaking was experienced on 15 January 1934 during an M_w = 8.1 earthquake (Hough and Bilham, 2008). The 1934 earthquake had a maximum intensity of X on the MMI scale in the Kathmandu Valley and destroyed about 19% and damaged about 38% of the buildings in the valley (Pandey and Molnar, 1988; Rana, 1935). On the other hand, the historical record of earthquake occurrences in the Himalayan region reveals that four major destructive earthquakes of greater than *M*8.0 have occurred in the region in 1897, 1905, 1934 and 1950 (Ambraseys and Douglas, 2004; Seeber and Armbruster, 1981; Khattri, 1987; Molnar, 1990; Molnar and Pandey, 1989; Hough and Bilham, 2008; Yeats and Lillie, 1991; and Yeats *et al.*, 1992). As shown in Fig. 1, however, the central part of the Himalayas has had no release of energy for a long period of time, which Khattri (1987) identified as a region of a seismic gap. Many other researchers, such as Bilham *et al.* (1995), Pandey *et al.* (1995), Pandey *et al.* (1999), have also warned that this particular region is a potential location for the next big earthquake in the Himalayas. Although the available historical record is inadequate for an accurate prediction of the recurrence period of great earthquakes in Nepal, the accessible data indicate that an earthquake of greater than *M*8.0 occurs at an interval of about 100 years. As it is already about 80 years from the 1934 Great Earthquake in Nepal, the threat of a major earthquake in the region, particularly in the Nepal Himalaya, in the next few decades is increasing. In 2002, the Japan International Cooperation Agency (JICA) conducted a loss estimation study in the Kathmandu Valley and predicted that the next major earthquake in Nepal might cause tens of thousands of deaths and nearly a hundred thousand injuries in the valley alone, particularly due to the potential for complete destruction of 59,000 houses and buildings.

Several studies reaffirm the fact that comparatively heavy earthquake damage in the Kathmandu Valley is associated with the valley ground structure (Hough and Bilham, 2008; Pandey and Molnar, 1988; Mugnier *et al.*, 2011). Geological exploration has revealed that the Kathmandu Valley is an ancient lake deposit, which measures several hundred meters at the deepest point and is made up of thick layers of clay, silt, sand, and gravel

Correspondence to: Youb Raj Paudyal, Geo-disaster Research Laboratory, Graduate School of Science and Engineering, Ehime University, Bunkyo-3, Matsuyama 790-8577, Japan
Tel: +81-89-927-8566; Fax: +81-89-927-8566
E-mail: youbrajpaudyal@gmail.com
[†]Graduate Student; [‡]Professor; [§]Doctor

Received December 27, 2011; **Accepted** March 27, 2012

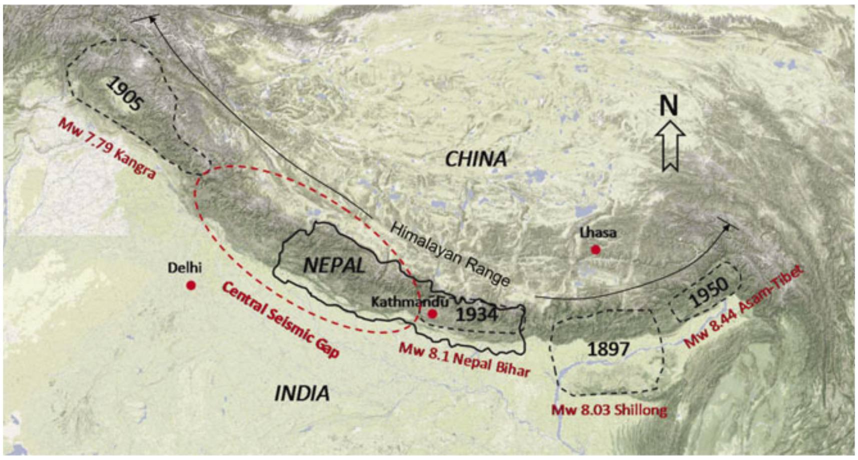

Fig.1 Distribution of probable rupture zones of the 1897, 1905, 1934 and 1950 earthquakes along the Himalayan arc. Modified after Yeats and Lillie (1991) and Yeats *et al.* (1992) and base map is taken from Google Terrain Map (2011)

in irregular layers of deposition ranging in age from the late Pliocene era to the present (Dongol, 1985; Fujii and Sakai, 2002; Moribayashi and Maruo, 1980; Sakai *et al.*, 2001; Yoshida and Igarashi, 1984; and Dahal and Aryal, 2002). Based on a gravity measurement study, Moribayashi and Maruo (1980) have estimated the maximum depth of the Kathmandu basin-fill sediments to be about 650 m. In the central part of the valley, however, a drill-well was found to hit the basement rock at a depth of about 550 m (Fujii and Sakai, 2002). On the other hand, based on previous studies as well as paleoclimatic study of the Kathmandu Basin conducted by Sakai *et al.* (2001), Sakai (2001) has divided the valley sediments into three groups: (1) marginal fluvio-deltaic facies in the northern part, (2) open lacustrine facies in the central part, and (3) alluvial fan facies in the southern part, as shown in Fig. 2. Based on the evidence of buildings damaged in the valley during past earthquakes, Dixit *et al.* (1998), Hough and Bilham (2008), and Mugnier *et al.* (2011) have mentioned that the valley is characterized by strong site effects. The basin sediment thickness and material properties vary from place to place, which may cause trapping and focusing of seismic waves during an earthquake, leading to an evident change in resonant frequency over short distances. The resonant frequency of a site is particularly important because it indicates the frequency of the spectrum under which the near-surface soft sediment amplifies the earthquake ground motion. This particular phenomenon is known as the site effect, which is generally studied through borehole with PS logging, strong ground motion analysis, microtremor data analysis, etc. In the context of the Kathmandu Valley, however, boreholes with PS logging method and strong ground motion analysis are not feasible, mainly because of the cost involved and unavailability of the strong ground motion data recording system in the required site. In this situation, the microtremor analysis may be a good option for the study of site effects in the Kathmandu Valley.

The microtremor analysis-based method for the site effects study was first introduced by Kanai (1957). Later, Nakamura (1989) improved this method, and now it has become widespread as a low-cost and effective tool to estimate the fundamental resonant frequency of sediments by measuring the microtremors at a single station. According to Nakamura (1989), the Horizontal-to-Vertical spectral (*H/V*) ratio is the Quasi Transfer Spectra (Transfer Function) of the soil strata over bedrock, which is obtained by taking the spectral ratio of the horizontal to vertical component of ground motion at a single station. In his paper, Nakamura (1989) brilliantly explains the use of this technique and gives a detailed explanation of the subsequent assumptions.

The Horizontal-to-Vertical spectral (*H/V*) ratio method has been widely applied in the last two decades for the study of site effects in different geographical and geological regions of the world. The elaborated discussion, applications, validations and limitations about the *H/V* method have come from many researchers, such as Bonnefoy-Claudet *et al.* (2006a, 2006b), Delgado *et al.* (2000), Field and Jacob (1993), Field *et al.* (1995), Gosar (2007), Gosar and Martinec (2009), Guo *et al*. (2002), Hardesty *et al.* (2010), Hung and Teng (1999), Lachet *et al.* (1996), Langston *et al.* (2009), Lermo and Chávez-García (1993), Lermo and Chávez-García (1994), Mucciarelli (2011), Parolai *et al.* (2004), Sánchez-Sesma *et al.* (2011), Toshinawa *et al.* (1997), Theodualidis *et al.* (2005), Tuan *et al.* (2011), Walling *et al.* (2009), Wen *et al*. (2011), Woolery *et al.* (2009), and Zandieh and Pezeshk (2011). These studies conclude that the microtremor *H/V* spectral ratios provide a reliable estimate of the resonance frequencies of soft soil deposits. Moreover, D'Amcio *et al.* (2004), Delgardo *et al.* (2000), Dinesh *et al.* (2010), Gosar and Lenart (2010), Ibs-von Seht and Wohlenberg (1999), Özalaybey *et al.* (2011), Parolai *et al.* (2002), Sukumaran

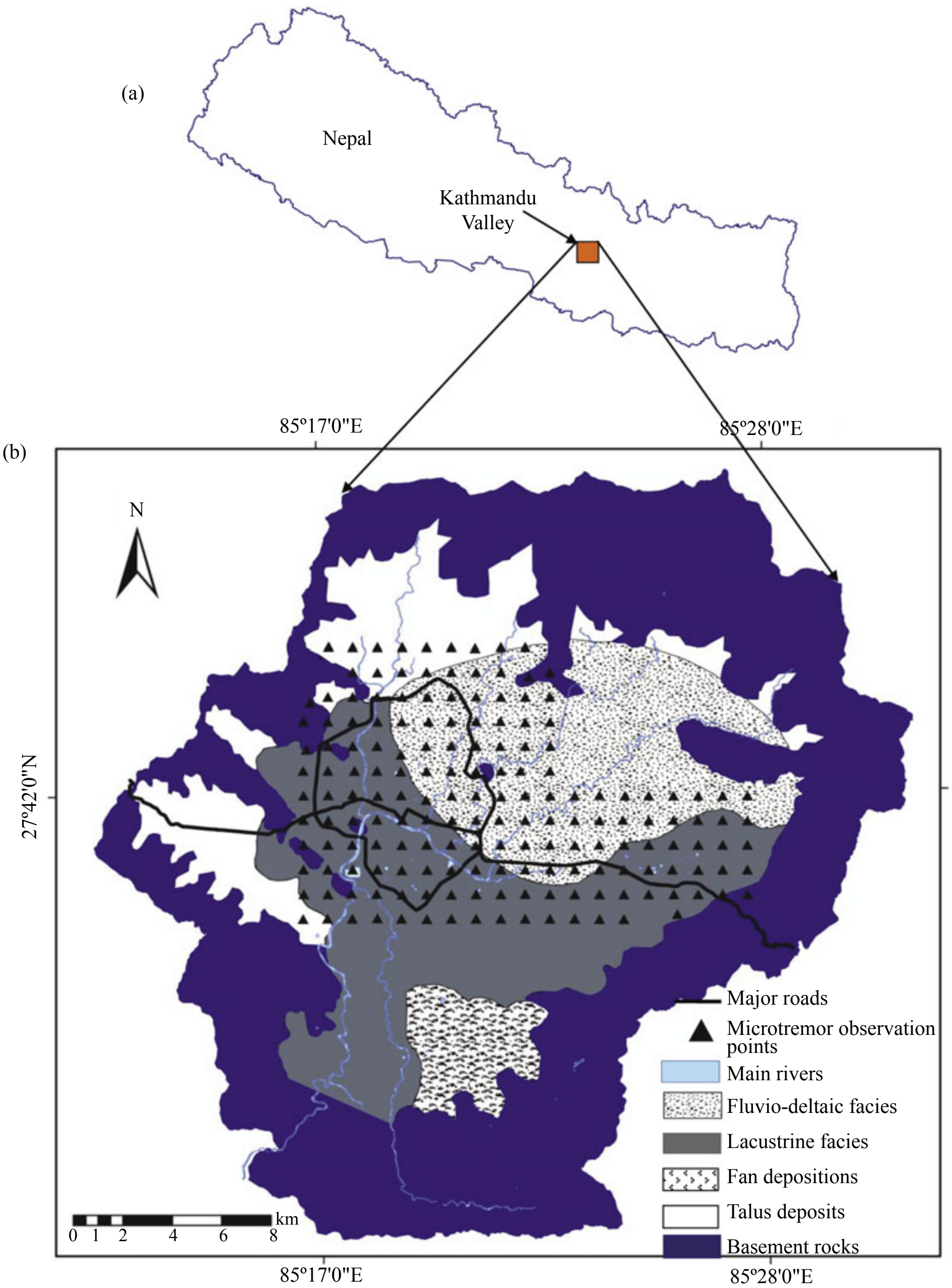

Fig. 2 Location map of the study area, (a) Map of Nepal and location of the Kathmandu Valley; (b) Geology of the Kathmandu Valley (redrawn after Shakai *et al.*, 2001) and microtremor observation points.

et al. (2011) have demonstrated that there is a strong correlation between shear wave velocity, resonance frequency and thickness of the sediments. They also give a very useful relationship between these parameters using the *H/V* method for different geographical and geological regions of the world.

Most of the past studies have revealed that the distribution of earthquake damage in a particular area is correlated with its fundamental frequency (e.g., Gosar, 2007; Teves-Costa *et al.*, 2007). However, some studies also indicate that depending upon the soil conditions of underlain strata, a second amplified frequency is locally revealed, which can play an important role in creating a resonance with the structures built over the ground during an earthquake (such as Fäh *et al.*, 1994; Toshinawa *et al.*, 1997; Guéguen *et al.*, 1998, 2000). As mentioned previously, the geological structure and sediment depositional environment in the Kathmandu Valley consists of many strata of sand, silt and clay sediments, which bring forward a possibility that two or more amplified frequencies occur during an earthquake. As the valley accommodates a number of low-rise to medium-rise buildings, historically important places and monuments, there are possibilities during an earthquake that the multiple amplified frequency may cause a resonance with structures in a broad frequency range, leading to an enhanced vibration of the structures and possible collapse. Therefore, in this study, an attempt has been made to investigate the response of the surface and the underneath layer during earthquakes using the Horizontal-to-Vertical spectral (*H/V*) ratio method. The main objective of this work is to delineate the area of single and multiple resonance frequencies in the Kathmandu Valley. More specifically, the paper focuses on the ground response in the areas which show multiple amplified frequencies and the thickness of the responsible surface soil layer is calculated for the amplification of seismic waves.

2 Data acquisition and analysis

The microtremor observations were made at a total of 172 nodal points in a 1-km grid covering about 210 km^2 area in the Kathmandu Valley, as shown in Fig. 2. The main source of microtremors in the valley could be vehicular movement that takes place almost 24 h in the cities of Kathmandu, Lalitpur and Bhaktapur, and the industrial facilities in and around the valley. Other possible sources of microtremors could also be human activities (construction activities, etc.), and the effects of winds on trees and buildings within the valley. A portable velocity sensor called New PIC was used to measure the microtremors, which is capable of recording three components of vibration: two horizontal, i.e., east-west and north-south, and one vertical. At each grid node, the microtremor data were recorded for 300 s at a sampling frequency of 100 Hz (i.e., 30,000 samples at each point), and were then plotted in terms of velocity-time histories. Each component of the recorded signal was corrected by the base line and divided into 15 windows of 2,048 samples (i.e., equivalent to 20.48 s), as illustrated in Fig. 3.

The influence of transient signals was minimized by taking 10–14 windows, with little or no transient signals, and Fourier analysis was carried out separately for each window using the Fast Fourier Transform (FFT) computer program to obtain the Fourier spectra. Then, the Fourier spectra were smoothed by the Parzen window at a bandwidth of 0.5 Hz. The average spectral ratio of the horizontal component of vibration to vertical (i.e., *H/V*) in each window was derived from Eq. (1) (Delgado *et al.*, 2000).

$$H/V = \sqrt{\left(F_{\mathrm{NS}}^2 + F_{\mathrm{EW}}^2\right)\Big/\left(2F_{\mathrm{UD}}^2\right)} \tag{1}$$

Here, F_{NS}, F_{EW} and F_{UD} are the Fourier amplitude spectra in the North-South (NS), East-West (EW) and Up-Down (UD) directions, respectively.

After deriving the *H/V* spectral ratios for all windows of record on a point, the *H/V* ratio for each particular point was obtained by averaging all those spectral ratios. The frequency of the site was obtained based on the observed peak in the *H/V* spectral ratio, which according to Bonnefoy-Claudet *et al.* (2006b), Field and Jacob (1993), and SESAME (2004), corresponds to the fundamental frequency or first resonant frequency of the site.

In order to calculate the thickness of a sediment layer over the bedrock or the thickness of the top soil layer, Kramer (1996) has derived an equation for one dimensional (1D) ground response analysis. According to his derivation, the 1D resonance frequency, denoted by f_0, is defined as the function of S-wave velocity (V_s) and the thickness *H* of the soil deposit, as in Eq. (2).

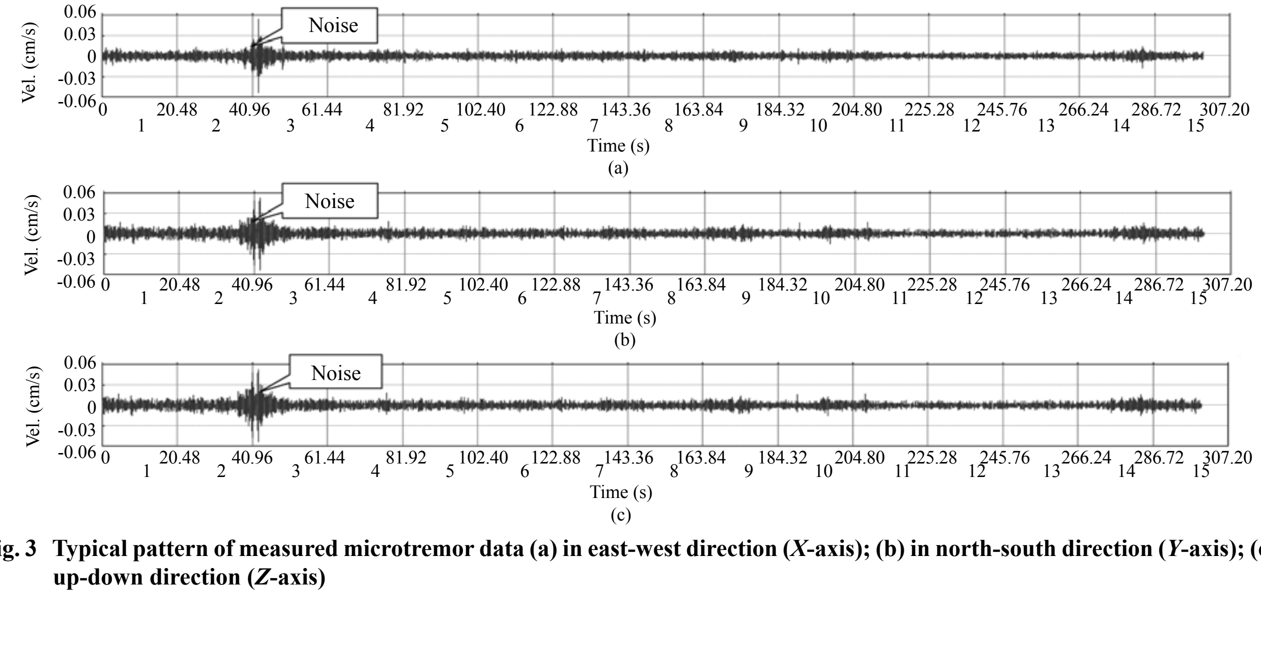

Fig. 3 Typical pattern of measured microtremor data (a) in east-west direction (*X*-axis); (b) in north-south direction (*Y*-axis); (c) in up-down direction (*Z*-axis)

$$f_0 = \frac{V_s}{4H} \tag{2}$$

In the case of a multi-stratified half-space (n layers), resonance frequency f_0 can be easily expressed by considering a single equivalent layer as follows.

$$f_0 = \frac{\sum_{i=1}^{n} V_{si} H_i}{4(\sum H_i)^2} \tag{3}$$

In this study, the thickness of the uppermost soil layer at an area of known shear wave velocity and resonance frequency is obtained through Eqs. (2) and (3).

3 Results and discussion

3.1 Frequency distribution in the Kathmandu Valley

The results of the microtremor survey are expressed in terms of resonance frequency of the ground at each survey point, as typically shown in Figs. 4 (a) and 4(b). As seen in the figures, microtremor observation point P91 has a single amplified frequency, while microtremor observation point P82 has two amplified frequencies (refer to Fig. 6). Likewise, Fig. 5 shows the *H/V* spectral ratio versus frequency graphs and the multiple amplified frequencies for different areas in the Kathmandu Valley. Variations in the shapes of *H/V* curves can be easily

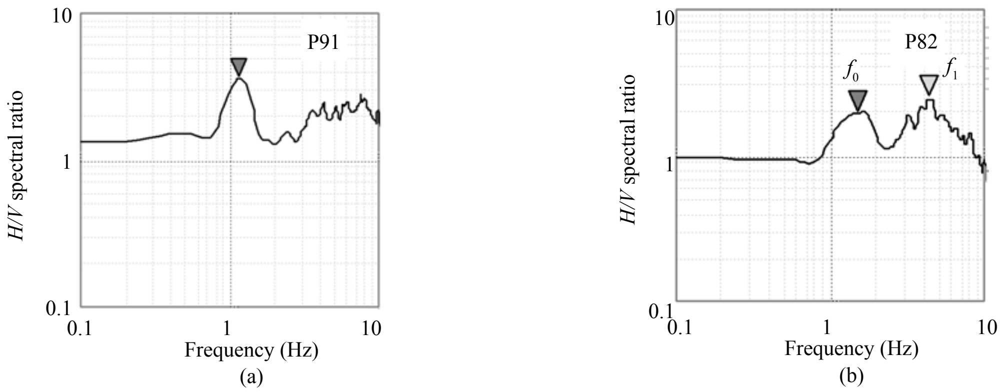

Fig. 4 (a) A typical single peak *H/V* spectral ratio; (b) A typical multiple peak *H/V* spectral ratio

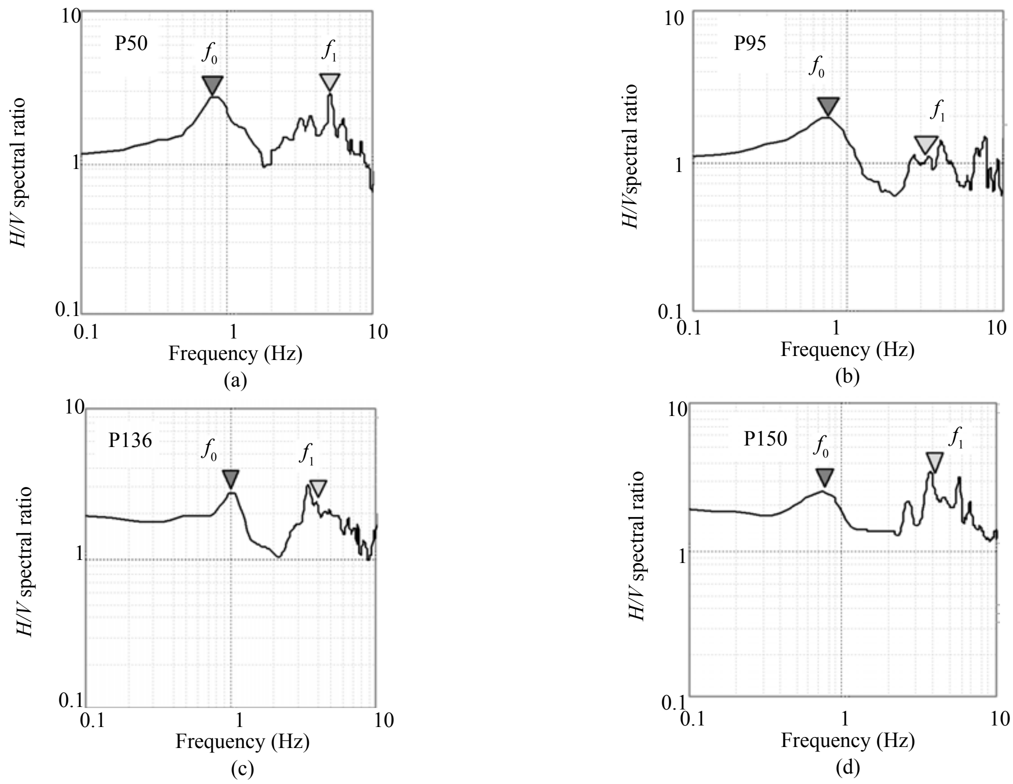

Fig. 5 Example of *H/V* spectral ratios with multiple amplified frequencies, triangles indicate the first and second resonant frequencies respectively

noticed in this figure. The first resonant frequency can be easily identified because the first peak is smoother than the second peak, but it may be difficult to exactly identify the second resonant frequency in the multiple-peak *H/V* spectral ratio curves. In order to identify the second resonant frequency at a particular location, a midpoint in the *H/V* curve with maximum amplitude is taken, but in some cases, the midpoint of the curve may not lie in the position of maximum amplitude. Both frequencies, i.e., first resonant frequency or predominant frequency and second resonant frequency as indicated by f_0 and f_1, as shown in Fig. 5, are representative of a particular site condition. The occurrence of the multiple peaks may be due to the presence of vertical heterogeneity in the soil column at that location, and they describe the overall seismic site response at two scales, including the deep and the upper soil profile response.

The microtremor analysis results show that about 80% of the measurement points in the study area exhibit single amplified frequencies that vary from 0.58 Hz to 8.9 Hz, whereas the remaining sites exhibit two amplified frequencies, in which the first amplified frequencies vary from 0.48 Hz to 1.52 Hz and the second amplified frequencies vary from 3.1 Hz to 7.5 Hz. Most of the *H/V* spectral ratios with multiple amplified frequencies lie in and around the central and northern part of the basin, which is dominated by the marginal fluvio-deltaic facies (river bed materials) (Sakai, 2001), and a few of them are found near the bank of the river and also in the areas consisting of organic clay with a sandy soil layer. A spatial distribution of single and multiple amplified frequencies in the study area is shown in Fig. 6. Only two multiple amplified frequency points (5 and 18) lie in Lalitpur City and 6 points (29, 43, 50, 53, 62 and 85) lie in the Bhaktapur City area. The remaining points lie in the Kathmandu City area where the population density is comparatively high (about 19,000 per km^2). This indicates that the Kathmandu City area has a wide range of resonance frequencies (i.e., 0.48 Hz to 8.9 Hz) than other areas of the valley. The Kathmandu Durbar Square area (a UNESCO cultural heritage site) is situated close to points 95 and 114. Similarly, the Bhaktapur Durbar Square area (an another UNESCO cultural heritage site) is situated very close to point 50. Both areas encompass temples of historical and cultural importance, archeologically important palace buildings, and the UNESCO-recognized world cultural heritage sites. Moreover, points 50, 79, 93, 94, 95, 96, 98, 114, 115, 116, 125, 127, 128, 136, 137, 149 and 150 (refer to Fig. 6) lie in highly commercial areas, and consist of very important structures such as multistory apartments, department stores, public places, government offices and old residential areas of the Kathmandu Valley. Similarly, points 131, 142, 143, 152, 153, 159, 160 and 170 (refer to Fig. 6) lie in the recently-urbanized area of the valley.

The distribution of the second peak resonant frequencies is mostly observed in the frequency range of 4 Hz to 6 Hz, as shown in Figs. 6 and 7(a), in the central

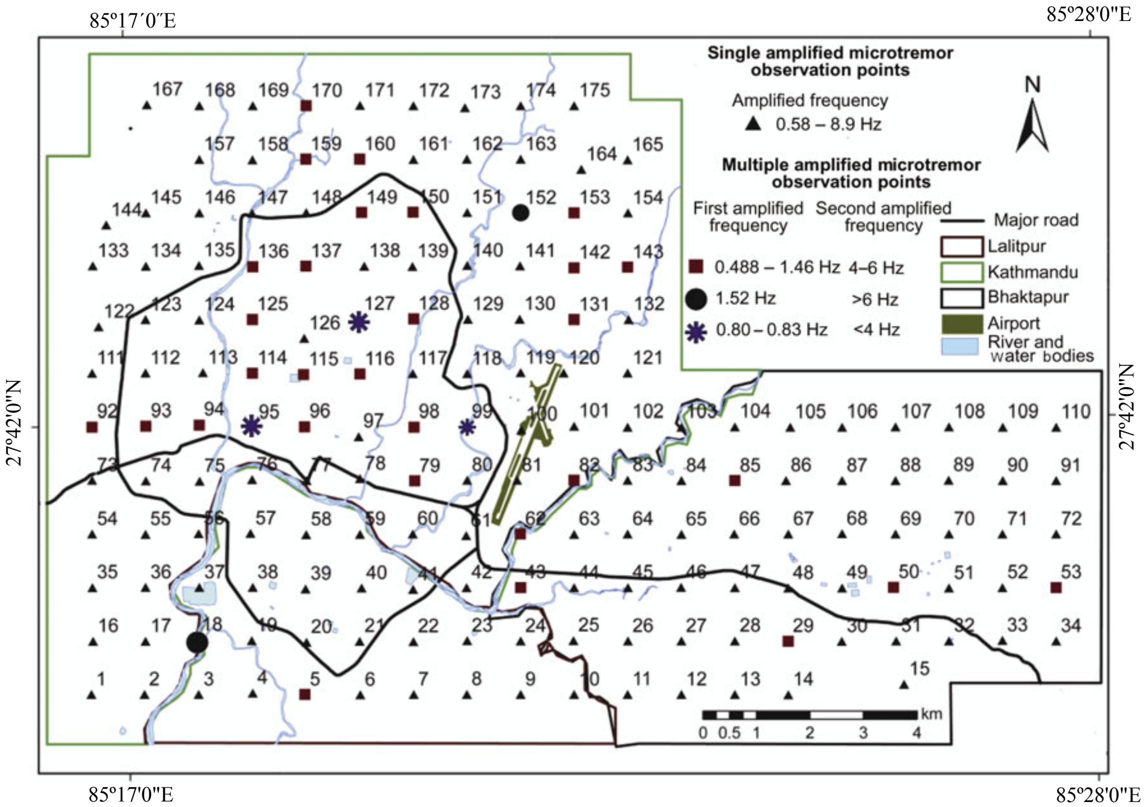

Fig. 6 Distribution of single and multiple resonance frequencies in the study area

and northern part of the valley, and also near the bank of the river. The ratio of second resonant frequencies to the first resonant frequencies is found to be approximately 5. The amplitude of the second peak frequencies vary from place to place, but are found higher than the amplitude of the first peak frequencies in most of the locations (Fig. 7b). These frequencies are linked with the presence of the surface layer. This indicates that the bottom strata of the surface layer should have a sufficient impedance contrast compared to the layer underneath. Most of the measurements in those locations were carried out in the night and morning times when the vehicle movement was very low, in order to minimize the effects of nearby noise. The distribution pattern of the *H/V* spectral ratios in the above areas shows that these second peak frequencies were not simply due to vehicle movement near the microtremor observation points. It consolidates the possibility that the second frequency peak could be due to the thin surface layer corresponding to the old alluvial deposits, which may behave as an independent structure in the soil column. This could have resulted from the presence of a stiff sediment layer, mainly composed of gravel and sand and presenting spatial and vertical heterogeneities. These results show two scales of amplification effects: (1) at low frequencies due to the global effect of the deep sedimentary basin, and (2) at high frequencies due to the uppermost surface layers (i.e., the consequences of the lacustrine and fluviatile deposit processes).

3.2 Estimation of soil layer thickness

Except for a countable number of boreholes drilled for the purpose of ground water exploration and investigation of soil parameters during building design, detailed geotechnical information of the deep structure of the Kathmandu Valley is not available. The shear wave velocity profile up to the basement rock is also not available. As a result, the correlation of fundamental frequency with sediment depth is not possible. However, there are five boreholes, as denoted by BH1, BH2, BH3, BH4 and BH5 in Fig. 8, in the valley where shear wave velocities were measured up to a depth of 30 m using PS logging by the Japan International Cooperation Agency in 2002 (JICA, 2002) during its study on Earthquake Risk Disaster Mitigation in the Kathmandu Valley.

In order to understand the level of impedance contrast and to determine the depth of the uppermost layer, which is responsible for the amplification of soil, a specific analysis was carried out of the soil profile and shear wave velocity of the boreholes, which are close to the two-peak *H/V* spectral ratio sites. As shown in Fig. 8, two double-peak *H/V* spectral ratio sites (i.e., point 50 and point 95) were found close to the JICA PS logging sites (i.e., BH5 and BH1). The *H/V* spectrum of Point 50, as shown in Fig. 5(a), has two peaks, which represent the multiple amplified frequencies at this point. Fig. 9(a) shows a soil profile, shear wave velocity profile and

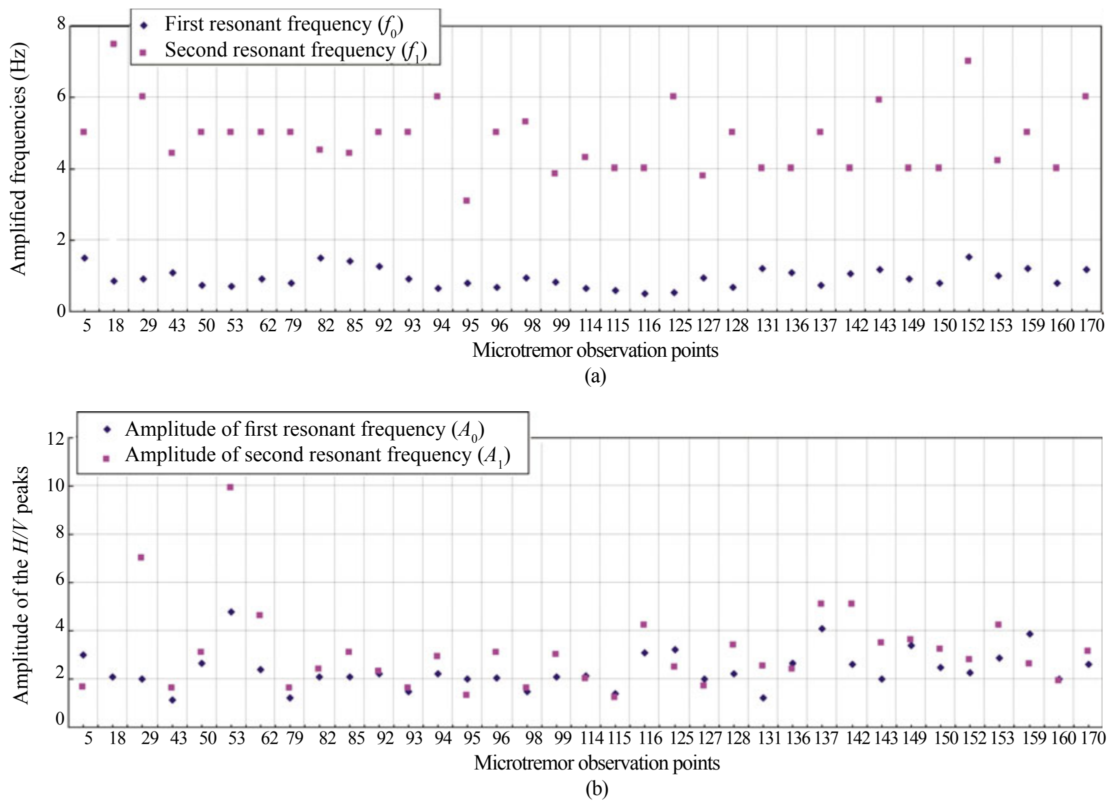

Fig. 7 (a) Distribution of multiple amplified frequencies in the study area; (b) Distribution of amplitude of multiple amplified frequencies in the study area

impedance ratio of the borehole BH5, which is close to the microtremor observation point 50 (refer to Fig. 8). Using 252.93 m/s as an average shear wave velocity in borehole BH5 (refer to Fig. 9(a); JICA, 2002) and the frequency of the second peak at microtremor observation point 50 (f_1=5.0 Hz), Eq. (2) yields a thickness of H_1 = 12.64 m, which is equal to the thickness of the uppermost layer in that area. The change in impedance contrast at various levels along the soil profile is clearly seen in Fig. 9(a), in which the maximum change in the impedance ratio is seen at a level of about 12.6 m from the surface and hence the strong impedance contrast (greater than 4) can be expected at that level. The calculated depth of the uppermost soil layer from the microtremor data analysis is found to be nearly equal to the depth of impedance contrast (refer to Fig. 9(a)), which shows good agreement between the calculated depth and the observed depth. Similarly, Fig. 5(b)) shows the *H/V* spectral ratio of Point 95, in which two peaks are seen, which represent the multiple amplified frequencies at this point. Using 188.86 m/s as an average shear wave velocity from the shear wave velocity profile for BH1 (Fig. 9(b); JICA, 2002) and the frequency (f_1 = 3.1 Hz) (refer to Fig. 5(b)) of the second peak observed near the borehole profile, Eq. (2) yields a thickness H_1 = 15.23 m, which is equal to the thickness of the uppermost layer in that location. Figure 9(b) shows the level of impedance contrast in which the change in impedance ratio is seen at about 17 m from the surface, which is nearly equal to the above calculated depth of the uppermost layer. The microtremor observation point 95 is about 300 m south of the borehole (i.e., BH1) location, and that may be the cause for the difference in calculated depth based on the microtremor data analysis with the depth of impedance contrast in the borehole profile.

Additionally, based on the shear wave velocity profile in all five sites (refer to Fig. 8), an average shear wave velocity up to a depth of 30 m for the Kathmandu Valley soil was obtained to be 246.87 m/s (JICA, 2002), while the second resonance frequency of the valley soil was mostly found to vary from 4 Hz to 6 Hz. Using this average shear wave velocity and the frequency of the second peak, the Eq. (2) yields a thickness of 10 m to 16 m, which is equal to the thickness of the uppermost layer of the Kathmandu Valley.

From the above results, it can be said that the valley areas, especially in the central and northern part, have a wider range of frequency than the other part of the valley. Based on the theoretical and numerical investigations, SESAME (2004), Toshinawa *et al.* (1997), and Guéguen *et al.* (1998) mention that two-peak *H/V* spectral ratio occurs due to two impedance contrasts, at two different scales: one for a thick structure, and the other for a shallow structure. Moreover, Lebrun *et al.* (2001) have shown in Grenoble (France) that the seismic ground motion is amplified in a wide frequency range due to the 2D or 3D effects and/or to the presence of an uppermost sediment layer. They also mention that the wide frequency range is due to the fluviatile deposits in the area and that the lateral variability can be strong from one

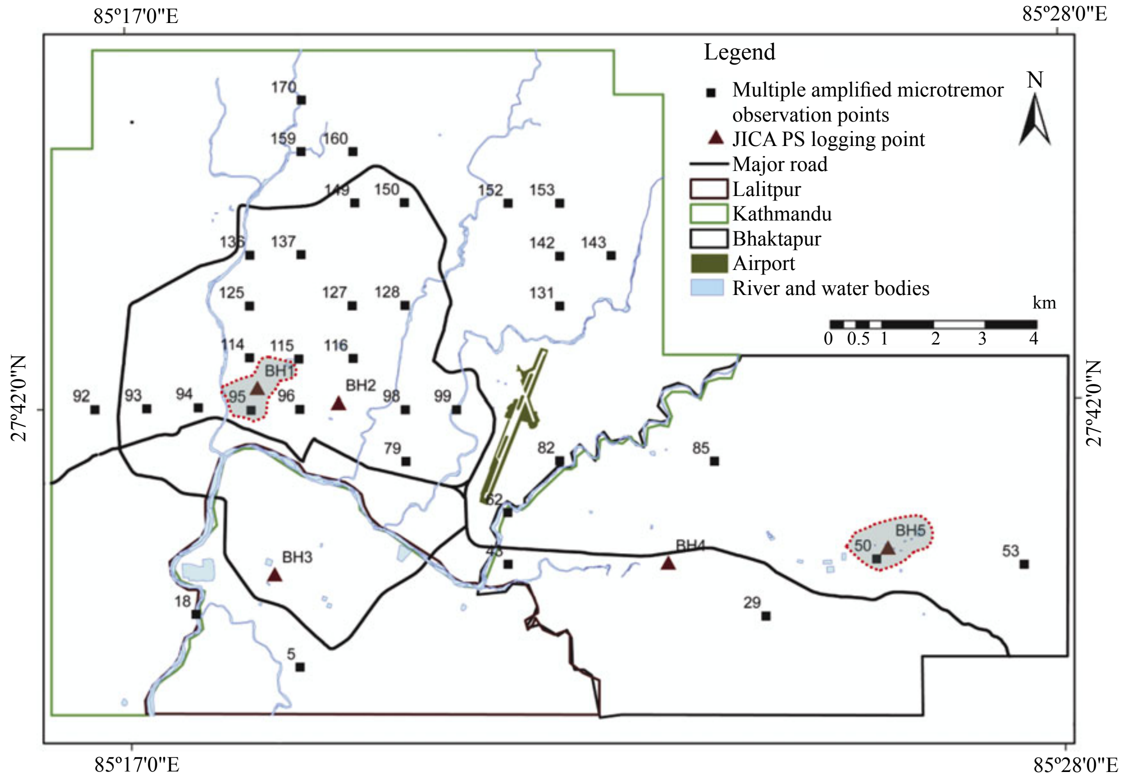

Fig. 8 Distribution of multiple amplified frequencies and location of JICA PS logging sites in study area, red dash boundary indicates the borehole and microtremor point taken for the analysis of depth of impedance contrast

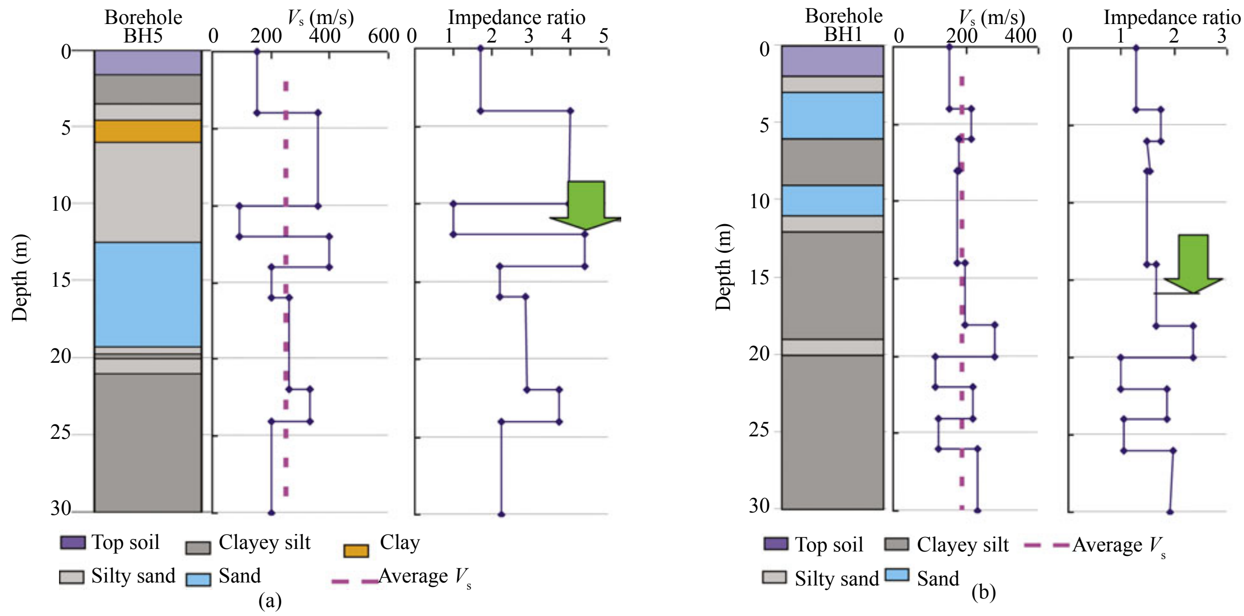

Fig. 9 Borehole profile, velocity profile and impedance ratio (a) in site BH5, and (b) in site BH1. Green downward arrows in (a) and (b) indicate the calculated depth of the top soil layer based on microtremor observation at Point 50 and Point 95 respectively (refer to Fig. 8)

point to another. In the Kathmandu Valley, the northern part generally consists of riverbed materials (Sakai, 2001). Due to the impedance contrast at a shallow depth, the uppermost layer behaves independently from the rest of the sediment-filled column. This assumption was also confirmed by simulation (2D-model) and experimental data (using Standard Spectral Ratio method) performed by Fäh *et al.* (1994) in the case of the Mexico Basin, where the second peak was attributed to the presence of a very soft uppermost clay layer resting on semi-infinite media.

The Kathmandu Valley accommodates a variety of buildings, especially in terms of building materials used and height (i.e., number of stories) of the structures. Most of the places consist of low-rise (1–5 stories) to medium-rise (6–10 stories) buildings. In general, Kramer (1996) has proposed that the fundamental frequency of an N-story building is approximately $10/N$ Hz, which results in an estimated predominant frequency of the Kathmandu Valley buildings to be around 1 Hz to 10 Hz. Moreover, the urban area mostly consists of 3 to 7 story buildings made of adobe, brick masonry and reinforced cement concrete. When the frequency of a building is equal or close to the frequency of the ground, resonance will take place, leading to an enhanced vibration of the structure and higher possibilities of collapse.

Finally, it can be said that the sediments in the Kathmandu Valley may cause two kinds of problems for the valley buildings during an earthquakes, especially in the central and northern part of the valley. One may be from the surface layer and other from the layer underneath. As higher resonant frequencies are characteristic to the surface sediment layer, this may mostly affect low-rise to medium-rise buildings, while the lower frequencies are characteristic of the layer underneath, which may affect medium-rise to high-rise buildings during an earthquake event.

4 Conclusion

Being a lacustrine basin with a complex depositional environment, the Kathmandu Valley has a wide range of sediment layers. As a result, there are inhomogeneities in the sediments, and their responses to seismic waves are different. In this study, the response of the surface and the underneath layer during an earthquake have been investigated using the Horizontal-to-Vertical spectral (H/V) ratio method of microtremor analysis. Single and multiple amplified frequencies were delineated based on the results of the microtremor observations at 172 points covering about 210 km^2. The investigation results have shown that two amplified frequencies appear on about 20% of the sites, which are mainly distributed in the central and the northern part of the basin. The predominant frequencies vary from 0.5 Hz to 8.9 Hz, whereas the second resonant frequencies vary mostly from 4 Hz to 6 Hz. These two resonance frequencies are characteristic of particular site conditions, and they describe the overall seismic site response in two scales, including the deep and surface soil layer. Depending upon the area, especially in the central and northern part, the top 10–20 m of the sediment layer plays an important role in making the second resonant effect in the basin.

The urban area of the Kathmandu Valley is mainly composed of low-rise to medium-rise buildings and/or improperly designed houses with high resonance frequencies as well as tall buildings with low resonance frequencies. The multiple amplified frequencies in a particular area can create a resonance effect both for low-rise as well as tall buildings. Therefore, the behavior of the surface layer as well as the layer underneath should be taken into consideration for seismic risk studies in the valley.

Acknowledgement

The authors are grateful to Mr. Ramhari Dahal (The Department of Education, Government of Nepal) and Mr. Prakash Poudyal (Kathmandu University) for their help during the extensive microtremor survey in the Kathmandu valley. The help provided by Ms. Manita Timilsina (PhD candidate, Graduate School of Science and Engineering, Ehime University) in preparing a few maps is greatly appreciated. The authors would also like to express their special appreciation to Dr. Shinichiro Mori (Associate Professor, Graduate School of Science and Engineering, Ehime University) for enabling the first author to analyze the microtremor survey data. The authors would also like to thank Ruth Vergin (Associate Professor, Ehime University) for help with the English. The authors also appreciate the comments and suggestions provided by three anonymous reviews, which helped us improve the clarity of this paper.

Finally, this is a part of the study entitled 'Integrated approach to studying rain- and earthquake-induced disasters in the Himalayan Watersheds and development of a strategic disaster education system' (Team Leader: Ryuichi Yatabe, Ehime University, AY2009~AY2011) and supported financially by the Government of Japan under Grant-in-Aid for Overseas Scientific Research and Investigation.

References

Ambraseys N and Douglas J (2004), "Magnitude Calibration of North Indian Earthquakes," *Geophysical Journal International*, **159**(1): 165–206.

Bilham R, Bodin P and Jackson M (1995), "Entertaining a Great Earthquake in Western Nepal: Historic Inactivity and Geodetic Tests for the Present State of Strain," *Journal of Nepal Geological Society,* **11**: 73–78.

Bonnefoy-Claudet S, Cotton F and Bard PY (2006a), "The Nature of Noise Wavefield and Its Applications for Site Effects Studies: A Literature Review," *Earth-Science Reviews*, **79**: 205–227.

Bonnefoy-Claudet S, Cornou C, Bard PY, Cotton F, Moczo P, Kristek J and Fäh D (2006b), "H/V Ratio: a Tool for Site Effects Evaluation Results from 1-D noise Simulations," *Geophysical Journal International,* **167**: 827–837.

Chitrakar GR and Pandey MR (1986), "Historical Earthquakes of Nepal," *Bulletin Geological Society of Nepal*, **4**:7–8.

Dahal RK and Aryal A (2002), "Geotechnical Properties of Soil of Sundhara and Jamal Area of Kathmandu," *Journal of Nepal Geological Society*, **27**(Special Issue):77–86.

D'Amico V, Picozzi M, Albarello D, Naso G and Tropenscovino S (2004), "Quick Estimates of Soft Sediment Thicknesses from Ambient Noise Horizontal to Vertical Spectral Ratios: a Case Study in Southern Italy," *Journal of Earthquake Engineering,* **8**(6): 895–908.

Delgado J, Casado CL, Lopez Giner J, Estevez A, Cuenca A and Molina S (2000), "Microtremors as a Geophysical Exploration Tool: Applications and Limitations," *Journal of Pure and Applied Geophysics,* **157**:1445–1462.

Dinesh BV, Nair GJ, Prasad AGV, Nakkeeran PV and Radhakrishna MC (2010), "Estimation of Sedimentary Layers Shear Wave Velocity Using Micro-tremor H/V Ratio Measurements for Bangalore City," *Soil Dynamics and Earthquake Engineering,* **30**:1377–1382.

Dixit A, Dwelly-Samant L, Nakarmi M, Pradhanang S and Tucker B (1998), "The Kathmandu valley Earthquake management plan," Published by National Society for Earthquake Technology-Nepal, pp. 38. http://www.preventionweb.net/english/professional/publications/v.php?id=1496.

Dongol GMS (1985), "Geology of the Kathmandu Fluvio-Lacustrine Sediments in the Light of New Vertebrate Fossil Occurrences," *Journal of Nepal Geological Society*, **3**: 43–47.

Fäh D, Suhadolc P, Mueller St and Panza GF (1994), "A Hybrid Method for the Estimation of Ground Motion in Sedimentary Basins: Quantitative Modeling for Mexico City," *Bulletin of the Seismological Society of America,* **84**: 383–99.

Field EH, Clement AC, Jacob KH, Aharonian V, Hough SE, Friberg PA, Babaian TO, Karapetian SS, Hovanessian SM and Abramian HA (1995), "Earthquake Site-response Study in Giuari (Formerly Leninakan) Armenia Using Ambient Noise Observations," *Bulletin of the Seismological Society of America*, **85**(1): 349–353.

Field E and Jacob K (1993), "The Theoretical Response of Sedimentary Layers to Ambient Seismic Noise," *Geophysical Research Letters,* **20**(24): 2925–2928.

Fujii R and Sakai H (2002), "Paleoclimatic Changes During the Last 25 Myr Recorded in the Kathmandu Basin Central Nepal Himalayas," *Journal of Asian Earth Sciences*, **20**: 255–266.

Gosar A (2007), "Microtremor HVSR Study for Assessing Site Effects in the Bovec Basin (NW Slovenia) Related to 1998 M_w 56 and 2004 M_w 52 Earthquakes," *Engineering Geology*, **91**: 178–193.

Gosar A and Lenart A (2010), "Mapping the Thickness of Sediments in the Ljubljana Moor Basin (Slovenia) Using Microtremors," *Bulletin of Earthquake Engineering*, **8**: 501–518.

Gosar A and Martinec M (2009), "Microtremor HVSR Study of Site Effects in the Ilirska Bistrica Town Area (S Slovenia)," *Journal of Earthquake Engineering*, **13**: 50–67.

Guéguen P, Chatelain JL, Guillier B and Yepes H (2000), "An Indication of the Soil Topmost Layer Response in Quito (Ecuador) Using Noise H/V Spectral Ratio," *Soil Dynamics and Earthquake Engineering*, **19**: 127–133.

Guéguen P, Chatelain J-L, Guillier B, Yepes H and Egred J (1998), "Site Effect and Damage Distribution in Pujili (Ecuador) after the 28 March Earthquake," *Soil Dynamics and Earthquake Engineering*, **17**: 329–334.

Guo X, Wong YL and Yuan YF (2002), "Estimation of Damping Ratio of Soil Sites Using Microtremor," *Earthquake Engineering and Engineering Vibration*, **1**(1): 45-49.

Hardesty K, Wolf LW and Bodin P (2010), "Case History, Noise to Signal: A Microtremor Study at Liquefaction Sites in the New Madrid Seismic Zone," *Geophysics*, **75**(3): 83–90.

Hough SE and Bilham R (2008), "Site Response of the Ganges Basin Inferred from Re-evaluated Macroseismic Observations from the 1897 Shillong 1905 Kangra and 1934 Nepal Earthquakes," *Journal of Earth System and Science*, **117**: 773–782.

Huang HC and Teng TL (1999), "An Evaluation on H/V Ratio vs Spectral Ratio for Site Response Estimation Using the 1994 Northridge Earthquake Sequence," *Pure and Applied Geophysics*, **156**: 631– 649.

Ibs-von Seht M and Wohlenberg J (1999), "Microtremor Measurements Used to Map Thickness of Soft Sediments," *Bulletin of the Seismological Society of America*, **89**: 250–259.

JICA (2002), *The Study on Earthquake Disaster Mitigation in the Kathmandu Valley Kingdom of Nepal*, Japan International Cooperation Agency (JICA) and Ministry of Home Affairs His Majesty's Government of Nepal, Volume I 2002, Summary p. 110, Volume III, Main Report 2/2, Earthquake Disaster Assessment and Data Base System, pp. 76.

Kanai K (1957), "The Requisite Conditions for Predominant Vibration of Ground," *Bulletin of Earthquake Research Institute,* University of Tokyo, **31**: 457.

Khattri KN (1987), "Great Earthquakes Seismicity Gaps and Potential for Earthquake Disaster along the Himalaya Plate Boundary," *Tectonophysics*, **138**: 79-92.

Kramer SL (1996), *Geotechnical Earthquake Engineering*, Chapter 7 and 8, Pearson Education Inc.

Lachet C, Bard PY, Hatzfeld D, Theodulidis N, Papaioannou C and Savvaidis A (1996), "Site Effects and Microzonation in the City of Thessaloniki (Greece) Comparison of Different Approaches," *Bulletin of the Seismological Society of America*, **67**: 713–724.

Langston CA, Chiu Shu-Chioung C, Lawrence Z, Bodin P and Horton S (2009), "Array Observations of Microseismic Noise and the Nature of H/V in the Mississippi Embayment," *Bulletin of the Seismological Society of America*, **99**(5): 2893-2911.

Lebrun B, Hatzfeld D and Bard PY (2001), "A Site Effect Study in Urban Area: Experimental Results in Grenoble (France)," *Pure and Applied Geophysics*, **158**: 2543–2557.

Lermo J and Chávaz-García FJ (1993), "Site Effect Evaluation Using Spectral Ratios with Only One Station," *Bulletin of the Seismological Society of America*, **83**: 1574–1594.

Lermo J and Chávaz-García FJ (1994), "Are Microtremors Useful in Site Response Evaluation," *Bulletin of the Seismological Society of America*, **84** (5): 1350–1364.

Molnar P (1990), "A Review of the Seismicity and the Rates of Active Underthrusting and the Deformatation at the Himalaya," *Journal of Himalayan Geology*, **1**: 131–154.

Molnar P and Pandey MR (1989), "Rupture Zones of Great Earthquakes in the Himalayan Region," *Proc. Ind. Acad. Sci.* (*Earth. and Plan. Sci.*), **98**: 61–70.

Moribayashi S and Maruo Y (1980), "Basement Topography of the Kathmandu Valley Nepal- An Application of the Gravitational Method to the Survey of a Tectonic Basin in the Himalaya," *Journal of Japan Society of Engineering Geology*, **21**: 30–37.

Mucciarelli M (2011), "Ambient Noise Measurements Following the 2011 Christchurch Earthquake: Relationships with Previous Microzonation Studies, Liquefaction, and Nonlinearity," *Seismological Research Letters*, **82**(6): 919–926.

Mugnier JL, Huyghe P, Gajurel AP, Upreti BN and Jouanne F (2011), "Seismites in the Kathmandu Basin and Seismic Hazard in Central Himalaya," *Tectonophysics*, **509** (1-2): 33–49.

Nakamura Y (1989), "A Method for Dynamic Characteristics Estimation of Subsurface Using Microtremor on the Ground Surface," *Quarterly Report of the Railway Technical Research Institute*, **30**(1): 25–33.

Özalaybey S, Zor E, Ergintav S and Tapırdamaz MC (2011), "Investigation of 3-D Basin Structures in the zmit BayArea (Turkey) by Single-station Microtremor and Gravimetric Methods," *Geophysical Journal International,* **186**: 883–894.

Pandey MR and Molnar P (1988), "The Distribution of Intensity of the Bihar-Nepal Earthquake 15 January 1934 and Bounds of the Extent of the Rupture Zone," *Journal of Nepal Geological Society*, **5**: 22–44.

Pandey MR, Tandukar RP, Avouac JP, Lavé J and Massot JP (1995), "Interseismic Strain Accumulation on the Himalayan Crustal Ramp (Nepal),” *Geophysical Research Letters*, **22**(7): 751–754.

Pandey MR, Tandukar RP, Avouac JP, Vergne J and Héritier Th (1999), “Seismotectonics of the Nepal Himalaya from a Local Seismic Network,” *Journal of Asian Earth Sciences*, **17**: 703–712.

Parolai S, Bormann P and Milkereit C (2002), “New Relationship between Vs Thickness of Sediments and Resonance Frequency Calculated by the H/V Ratio of Seismic Noise for the Cologne Area (Germany),” *Bulletin of the Seismological Society of America*, **92**(6): 2521–2527.

Parolai S, Richwalski SM, Milkereit C and Bormann P (2004), “Assessment of the Stability of H/V Spectral Ratios from Ambient Noise and Comparison with Earthquake Data in the Cologne Area (Germany),” *Tectonophysics,* **390**: 57–73.

Rana BJB (1935), *Nepal Ko Maha Bhukampa* (*Great Earthquake of Nepal*), Jorganesh Press.

Sakai H (2001), “Stratigraphic Division and Sedimentary Facies of the Kathmandu Basin Group, Central Nepal,” *Journal of Nepal Geological Society*, **25** (Special Issue): 19–32.

Sakai H, Fujii R, Kuwahara Y, Upreti BN and Shrestha SD (2001), “Core Drilling of the Basin-fill Sediments in the Kathmandu Valley for Paleoclimatic Study: Preliminary Results,” *Journal of Nepal Geological Society*, **25**(Special Issue): 9-18.

Sánchez-Sesma FJ, Rodríguez M, Iturrarán-Viveros U, Luzón F, Campillo M, Margerin L, García-Jerez A, Suarez M, Santoyo MA and Rodríguez-Castellanos A (2011), “A Theory for Microtremor H/V Spectral Ratio: Application for a Layered Medium,” *Geophysical Journal International*, **186**: 221–225.

Seeber L and Armbruster J (1981), “Great Detachment Earthquakes along the Himalaya Arc and Long Term Forecasts” DW Simpson and PG Richards (Eds), *Earthquake Prediction*: *An International Review*, *Maurice Ewing Series,* American Gephysical Union Washington D C, **4**: 259–277.

SESAME (2004), *Guidelines for the Implementation of the h/v Spectral Ratio Technique on Ambient Vibrations Measurements Processing and Interpretation*, SESAME European Research Project, Wp12 –Deliverable d2312 European Commission – Research General Directorate, Project No. EVG1-CT-2000-00026.

Sukumaran P, Parvez IA, Sant DA, Rangarajan G and Krishnan K (2011), “Profiling of Late Tertiary–Early Quaternary Surface in the Lower Reaches of Narmada Valley Using Microtremors,” *Journal of Asian Earth Sciences,* **41**: 325–334.

Teves-Costa P, Oliveira CS and Senos ML (2007), “Effects of Local Site and Building Parameters on Damage Distribution in Angra do Heroísmo—Azores,” *Soil Dynamics and Earthquake Engineering*, **27**: 986–999.

Theodulidis N, Panou AA, Hatzidimitriou P, Stylianidis K and Papazachos CB (2005), “Ambient Noise Horizontal-to-vertical Spectral Ratio in Site Effects Estimation and Correlation with Seismic Damage Distribution in Urban Environment: the Case of the City of Thessaloniki (Northern Greece),” *Soil Dynamics and Earthquake Engineering*, **25**: 261–274.

Toshinawa T, Taber JJ and Berril JB (1997), “Distribution of ground Motion Intensity Inferred from Quationnaire Survey Earthquake Recordings and Microtremors Measurements-a Case Study in Christchurch New Zealand During the Arthurs Pass Earthquake,” *Bulletin of seismological Society of America*, **87**: 356–369.

Tuan TT, Scherbaum F and Malischewsky PG (2011), “On the Relationship of Peaks and Troughs of the Ellipticity (H/V) of Rayleigh Waves and the Transmission Response of Single Layer over Half-space Models,” *Geophysical Journal International*, **184**: 793–800.

Walling MY, Mohanty WK, Nath SK, Mitra S and John A (2009), “Microtremor Survey in Talchir India to Ascertain Its Basin Characteristics in Terms of Predominant Frequency by Nakamura’s Ratio Technique,” *Engineering Geology*, **106**: 123–132.

Wen RZ, Ren YF and Shi DC (2011), “Improved HVSR Site Classification Method for Free-field Strong Motion Stations Validated with Wenchuan Aftershock Recordings,” *Earthquake Engineering and Engineering Vibration*, **10**: 325–337.

Woolery EW, Street R, and Hart P (2009), “Evaluation of Linear Site Response Methods for Estimating Higher-Frequency (>2Hz) Ground Motions in the Lower Wabash River Valley of the Central United States,” *Seismological Research Letter*, **80**: 525–538.

Yeats RS and Lillie RJ (1991), “Contemporary Tectonics of the Himalayan Frontal Fault System: Folds Blind Thrusts and the 1905 Kangra Earthquake,” *Journal of Structural Geology*, **13**: 215–225.

Yeats RS, Nakata T, Farah A ,Fort M, Mirza MA, Pandey MR and Stein RS (1992), “The Himalayan Frontal Fault Sytem,” *Annales Tectonicae,* **6**(Special Issue): 85–98.

Yoshida M and Igarashi Y (1984), “Neogene to Quaternary lacustrine sediemnts in the Kathamandu Valley, Nepal,” *Journal of Nepal Geological Society*, 4: 73–100.

Zandieh A and Pezeshk S (2011), “A Study of Horizontal-to-Vertical Component Spectral Ratio in the New Madrid Seismic Zone,” *Bulletin of the Seismological Society of America*, **101**(1): 287–296.